Cascaded Real-Time Kinematic Positioning with Multi-Frequency Linear Combinations

Patrick Henkel and Christoph Günther
Technische Universität München
Arcisstrasse 21
80333 München, Germany
{patrick.henkel, christoph.guenther}@tum.de

***Abstract*—Real-Time Kinematic (RTK) positioning with Global Navigation Satellite Systems (GNSS) enables centimeter-level positioning accuracies. However, the small wavelength of the GNSS carrier signals often prevents a reliable ambiguity resolution.**

This paper proposes a cascaded RTK positioning with multi-frequency linear combinations. The combinations are characterized by a large wavelength, which enables a robust ambiguity resolution even in the presence of uncorrected geometric and ionospheric biases at the price of a slightly increased noise level.

***Keywords*—RTK; Multi-frequency combinations**

I. Introduction

The GNSS carrier phase measurements can be tracked with millimeter- to centimeter-level accuracy. However, the carrier phase is periodic with a wavelength of only 19 cm, which results in an integer ambiguity for each satellite. The reliability of the ambiguity fixing is typically limited by uncorrected biases as described by Teunissen in [1]. Linear combinations of carrier phase measurements with a wavelength of several meters were derived in [2] to improve the robustness of ambiguity resolution. This paper provides a cascaded RTK positioning with optimized multi-frequency linear combinations.

II. Multi-Frequency Phase Combinations

In this section, we introduce the measurement models and constraints for multi-frequency linear combinations for Real-Time Kinematic (RTK) positioning. The combinations are determined according to the following aspects:

- tropospheric, ionospheric and orbital errors are suppressed by differential measurements
- no inclusion of pseudorange measurements in multi-frequency combination to avoid multipath
- multi-frequency phase combinations designed primarily to increase wavelength and secondarily to reduce ionospheric errors

The double difference (DD) carrier phase measurement of a static receiver pair u and r and satellite pair k and l (the latter one serving as common reference satellite) on frequency $m \in \{1,\ldots,M\}$ at time t_j, $j \in \{1,\ldots,n\}$, is modeled according to [3] as

$$\begin{aligned}\lambda_m\varphi^{kl}_{ur,m}(t_j) &:= \lambda_m(\varphi^k_{u,m}(t_j)-\varphi^k_{r,m}(t_j)) \\ &\quad -\lambda_m(\varphi^l_{u,m}(t_j)-\varphi^l_{r,m}(t_j)) \\ &= (\vec{e}^{\,kl}_u)^{\mathrm{T}}\vec{b}_{ur}+\lambda_m N^{kl}_{ur,m}+\varepsilon^{kl}_{ur,m}(t_j),\end{aligned} \tag{1}$$

with wavelength λ_m, direction vector $\vec{e}^{\,k}_u = (\vec{x}_u - \vec{x}^{\,k})/\|\vec{x}_u - \vec{x}^{\,k}\|$ pointing from the satellite to the receiver, baseline vector $\vec{b}_{ur} = \vec{x}_u - \vec{x}_r$, receiver position $\vec{x}_u$, DD integer ambiguity $N^{kl}_{ur,m}$ and DD phase noise $\varepsilon^{kl}_{ur,m}$ including phase multipath. The DD pseudorange measurement is modeled similarly [3]:

$$\begin{aligned}\rho^{kl}_{ur,m}(t_j) &:= (\rho^k_{u,m}(t_j)-\rho^k_{r,m}(t_j))-(\rho^l_{u,m}(t_j)-\rho^l_{r,m}(t_j)) \\ &= (\vec{e}^{\,kl}_u)^{\mathrm{T}}\vec{b}_{ur}+\Delta\rho^{kl}_{\mathrm{MP},ur,m}(t_j)+\eta^{kl}_{ur,m}(t_j),\end{aligned} \tag{2}$$

with the DD pseudorange multipath error $\Delta\rho^{kl}_{\mathrm{MP},ur,m}$ and the DD code noise $\eta^{kl}_{ur,m}$.

We perform a linear combination of the phase measurements on all frequencies $m \in \{1,\ldots,M\}$ and request that the multi-frequency combination can be expressed as

$$\begin{aligned}&\sum_{m=1}^{M}\alpha^i_m\lambda_m\varphi^{kl}_{ur,m}(t_j) \\ &\stackrel{!}{=} (\vec{e}^{\,kl}_u)^{\mathrm{T}}\vec{b}_{ur}+\lambda^i N^{kl,i}_{ur}+\sum_{m=1}^{M}\alpha^i_m\varepsilon^{kl}_{ur,m}(t_j),\end{aligned} \tag{3}$$

with the linear coefficient α^i_m, the wavelength λ^i and integer ambiguity $N^{kl,i}_{ur}$ of the i-th multi-frequency combination. This constraint is split into two constraints: The first constraint refers to the geometry, which should be preserved:

$$\sum_{m=1}^{M}\alpha^i_m \stackrel{!}{=} 1. \tag{4}$$

The 2nd constraint addresses the combination of ambiguities:

$$\sum_{m=1}^{M}\alpha^i_m\lambda_m N^{kl}_{ur,m} \stackrel{!}{=} \lambda^i N^{kl,i}_{ur}. \tag{5}$$

Dividing this equation by λ^i results in an integer equation. The equation should be fulfilled for any unknown $N^{kl}_{ur,m}$, which leads to the integer constraint:

$$n^i_m := \frac{\alpha^i_m\lambda_m}{\lambda^i} \stackrel{!}{\in} \mathbb{Z}. \tag{6}$$

We solve this equation for α^i_m, plug the result into the geometry-preserving constraint of Eq. (4) and solve it for λ^i to obtain the wavelength of the combination:

$$\lambda^i = \frac{1}{\sum_{m=1}^{M}\frac{n^i_m}{\lambda_m}}. \tag{7}$$

The combination scales the DD ionospheric delay by $\alpha_{\mathrm{I}}^i = \sum_{m=1}^{M} \alpha_m^i f_1^2/f_m^2$ and amplifies the noise standard deviation by $\alpha_{\mathrm{n}}^i = \sqrt{\sum_{m=1}^{M}(\alpha_m^i)^2}$ assuming an equal noise standard deviation on each frequency.

III. Search of combinations

The coefficients of the multi-frequency phase combinations are determined by a numerical search. We applied the following three different sets of criteria:

- widelane combinations ($\lambda^i > \max_m(\lambda_m)$) with low noise amplification ($n_{\max} = 1$) and acceptance of slight ionospheric amplification ($|\alpha_{\mathrm{I}}^i| < 2$)
- widelane combinations with large wavelengths ($\lambda^i > 1\mathrm{m}$), very limited amplification of ionospheric errors ($|\alpha_{\mathrm{I}}^i| < 1.1$) and moderate noise amplification ($n_{\max} = 10$)
- narrowlane combinations ($\lambda^i < \min_m(\lambda_m)$) with strong suppression of ionospheric errors ($|\alpha_{\mathrm{I}}^i| < 0.01$) and limited noise amplification ($n_{\max} = 5$)

The results are shown for Galileo triple frequency E1, E5b and E5a measurements in Tab. I in accordance with [2], whereby the combinations C1 to C3 refer to the first criterion, the combinations C4 to C9 to the second criterion, and the combinations C10 and C11 to the third criterion.

TABLE I. Selected triple-frequency phase-only combinations of Galileo measurements

Name	n_1^i E1	n_2^i E5b	n_3^i E5a	λ^i [m]	α_{I}^i	α_{n}^i
C1	0	1	-1	9.768	-1.748	54.923
C2	1	-1	0	0.814	-1.305	5.389
C3	1	0	-1	0.751	-1.339	4.928
C4	1	-10	9	3.256	0.023	175.237
C5	1	-9	8	2.442	-0.420	117.791
C6	1	-8	7	1.954	-0.686	83.343
C7	1	-7	6	1.628	-0.863	60.402
C8	1	-6	5	1.396	-0.989	44.047
C9	1	-5	4	1.221	-1.084	31.826
C10	4	-1	-2	0.109	0.010	2.493
C11	4	0	-3	0.108	-0.010	2.605

IV. Cascaded RTK positioning

A cascaded ambiguity resolution starts with the ambiguity fixing of a widelane combination with a large wavelength and, then, fixes the ambiguities of further linear combinations with successively smaller wavelengths and lower noise level [4]. The advantage of the cascaded ambiguity resolution is to obtain a faster fix and, thereby, a higher availability of a fixed solution than for uncombined measurements.

In this section, we describe a cascaded RTK positioning using some of the combinations from Tab. I. The proposed scheme includes 4 cascades:

1) Fixing of ambiguities of C1 combination by joint processing of code measurements and C1 combination
2) Fixing of ambiguities of C4 combination by joint processing of C1 and C4 combinations
3) Determination of ambiguities of C2 combination from linear combination of C1 and C4 ambiguities
4) Joint processing of C2 and C10 combinations for precise RTK positioning

The C1 combination (also referred to as super widelane combination) was chosen in the first cascade due to its large wavelength, which enables an almost instantaneous ambiguity resolution. In the second cascade, the C4 was selected since it has the largest wavelength and strongest ionospheric suppression in the second group of combinations. The third cascade includes the determination of the C2 ambiguities from a linear combination of C1 and C4 ambiguities, i.e. $N_{ur}^{\mathrm{C2}} = 9 \cdot N_{ur}^{\mathrm{C1}} + N_{ur}^{\mathrm{C4}}$. The C2 combination is attractive due its low noise amplification. In the 4-th cascade, the C10 combination is considered since it has an even lower noise amplification and strong ionospheric suppression. However, the small wavelength of this narrowlane combination implies that the respective ambiguities might be estimated only as float numbers.

In the first cascade, we consider the uncombined DD pseudorange measurements on all frequencies and the multi-frequency combination of the DD carrier phase measurements:

$$z^1(t_j) = \begin{pmatrix} \rho_{ur,1}(t_j) \\ \vdots \\ \rho_{ur,M}(t_j) \\ \sum_{m=1}^{M} \alpha_m^i \lambda_m \varphi_{ur,m}(t_j) \end{pmatrix}, \tag{8}$$

where $\rho_{ur,m}$ and $\varphi_{ur,m}$ are vectors of DD pseudorange and carrier phase measurements of all DDs, i.e.

$$\begin{aligned} \rho_{ur,m}(t_j) &= \left(\rho_{ur,m}^{1l}(t_j), \ldots, \rho_{ur,m}^{Kl}(t_j)\right)^{\mathrm{T}} \\ \lambda_m \varphi_{ur,m}(t_j) &= \left(\lambda_m \varphi_{ur,m}^{1l}(t_j), \ldots, \lambda_m \varphi_{ur,m}^{Kl}(t_j)\right)^{\mathrm{T}} \end{aligned} \tag{9}$$

In the second and all subsequent cascades, we consider two combinations of phase measurements: The first combination corresponds to the combination, that was used in the previous cascade. The respective ambiguities of this combination are also known from the previous cascade. The second combination is a new combination of the current cascade with unknown ambiguities. We stack both combinations in a single vector at cascade i, and use the fixed ambiguities $\check{N}_{ur}^{i-1}$ of the previous combination, i.e.

$$z^i(t_j) = \begin{pmatrix} \sum_{m=1}^{M} \alpha_m^{i-1} \lambda_m \varphi_{ur,m}(t_j) - \lambda^{i-1} \check{N}_{ur}^{i-1} \\ \sum_{m=1}^{M} \alpha_m^i \ \ \lambda_m \varphi_{ur,m}(t_j) \end{pmatrix} \forall\, i \geq 2, \tag{10}$$

where

$$N_{ur}^i = \left(\sum_{m=1}^{M} n_m^i N_{ur,m}^{1l}, \ldots, \sum_{m=1}^{M} n_m^i N_{ur,m}^{Kl} \right)^{\mathrm{T}}, \tag{11}$$

with n_m^i being defined in Eq. (6).

The number of unknown baseline coordinates, DD ambiguities and DD pseudorange multipath errors exceeds the number of available measurements in one epoch. Therefore, we consider the measurements of all epochs $j = \{1, \ldots, n\}$ at cascade i jointly in a single vector, i.e.

$$z^i = \left((z^i(t_1))^{\mathrm{T}}, \ldots, (z^i(t_n))^{\mathrm{T}}\right)^{\mathrm{T}}. \tag{12}$$

At the first cascade, we use an additional information on the pseudorange multipath errors, i.e. we model the time-difference of the pseudorange multipath errors as zero mean Gaussian noise with covariance matrix $\Sigma_{\Delta\rho_{\mathrm{MP},ur,m}}$:

$$\Delta\rho_{\mathrm{MP},ur,m}(t_j) - \Delta\rho_{\mathrm{MP},ur,m}(t_{j-1}) \sim \mathcal{N}\left(0, \Sigma_{\Delta\rho_{\mathrm{MP},ur,m}}\right), \tag{13}$$

with

$$\Delta\rho_{\mathrm{MP},ur,m}(t_j) = \left(\Delta\rho^{1l}_{\mathrm{MP},ur,m}(t_j), \ldots, \Delta\rho^{Kl}_{\mathrm{MP},ur,m}(t_j)\right)^{\mathrm{T}}.$$

The multipath constraint is helpful to improve the conditioning of the system of observation equations. The tightness of the constraint depends on the magnitude of $\Sigma_{\Delta\rho_{\mathrm{MP},ur,m}}$. We include the multipath constraints in the measurement vector at the first cascade by adding $M(n-1)$ zeros at the end, i.e.

$$z^1 = \left((z^1(t_1))^{\mathrm{T}}, \ldots, (z^1(t_n))^{\mathrm{T}}, 0^{1\times M(n-1)}\right)^{\mathrm{T}}. \tag{14}$$

The unknown parameters are stacked in a single vector ξ^i similar to the measurements. At the first cascade, the unknown parameters include the baseline coordinates, DD ambiguities and DD pseudorange multipath errors:

$$\xi^1 = \Big(\vec{b}^{\mathrm{T}}_{ur}, (N^i_{ur})^{\mathrm{T}}, \Delta\rho^{\mathrm{T}}_{\mathrm{MP},ur,1}(t_1), \ldots, \Delta\rho^{\mathrm{T}}_{\mathrm{MP},ur,M}(t_1), \ldots \Delta\rho^{\mathrm{T}}_{\mathrm{MP},ur,1}(t_n), \ldots, \Delta\rho^{\mathrm{T}}_{\mathrm{MP},ur,M}(t_n)\Big)^{\mathrm{T}} \tag{15}$$

The cascades $i \geq 2$ do not include any pseudorange measurements, i.e. the pseudorange multipath errors do not need to be estimated and the state vector simplifies to:

$$\xi^i = \left(\vec{b}^{\mathrm{T}}_{ur}, (N^i_{ur})^{\mathrm{T}}\right)^{\mathrm{T}} \quad \forall\, i \geq 2. \tag{16}$$

The DD carrier phase and pseudorange measurements of Eq. (1) and (2) are linear depend on the state parameters, i.e.

$$z^i = H^i \xi^i + \eta_{z^i}, \tag{17}$$

with H^i being the mapping matrix of the state parameters into measurement domain and $\eta_{z^i} \sim N(0, \Sigma_{z^i})$ including the pseudorange noise, combined phase noise and/ or the errors of the multipath constraints. The measurement covariance matrix of cascade $i \geq 2$ is further developed as

$$\Sigma_{z_i} = \mathrm{diag}\left(\Sigma_{z^i}(t_1), \ldots, \Sigma_{z^i}(t_n)\right), \tag{18}$$

with

$$\Sigma_{z^i}(t_j) = \begin{pmatrix} \sum_{m=1}^{M} (\alpha_m^{i-1})^2 \Sigma_{\lambda_m\varphi_{ur,m}} & \sum_{m=1}^{M} \alpha_m^{i-1}\alpha_m \Sigma_{\lambda_m\varphi_{ur,m}} \\ \sum_{m=1}^{M} \alpha_m^{i-1}\alpha_m \Sigma_{\lambda_m\varphi_{ur,m}} & \sum_{m=1}^{M} (\alpha_m^{i})^2 \Sigma_{\lambda_m\varphi_{ur,m}} \end{pmatrix}, \tag{19}$$

with $\Sigma_{\lambda_m\varphi_{ur,m}}$ being the covariance matrix of the uncombined DD phase measurements on frequency m.

The mapping matrix at the second and any later cascade is obtained from Eq. (1), (3), (9), (10), (12), (16) and (17) as

$$H^i = \left(\begin{array}{c|c} H(t_1) & 0^K \\ H(t_1) & \lambda^i\, I^K \\ \hline \vdots & \vdots \\ \hline H(t_n) & 0^K \\ H(t_n) & \lambda^i\, I^K \end{array}\right) \quad \forall\, i \geq 2, \tag{20}$$

with the identity matrix I^K with K rows and K columns, and the geometry matrix $H(t_j)$ being given by

$$H(t_j) = \begin{pmatrix} (\vec{e}^{\,1l}_u(t_j))^{\mathrm{T}} \\ \vdots \\ (\vec{e}^{\,Kl}_u(t_j))^{\mathrm{T}} \end{pmatrix}. \tag{21}$$

The state parameters are estimated by minimizing the sum of squared measurement residuals, i.e.

$$\begin{aligned} \hat{\xi}^i &= \arg\min_{\xi^i} \|z^i - H^i\xi^i\|^2_{\Sigma^{-1}_{z^i}} \\ &= \left((H^i)^{\mathrm{T}}\Sigma^{-1}_{z^i}H^i\right)^{-1}(H^i)^{\mathrm{T}}\Sigma^{-1}_{z^i}z^i. \end{aligned} \tag{22}$$

The float ambiguity estimates are included in $\hat{\xi}^i$ and can be extracted using Eq. (16), i.e.

$$\hat{N}^i_{ur} = \left(\hat{\xi}^i_{3+1}, \ldots, \hat{\xi}^i_{3+K}\right)^{\mathrm{T}} =: S\hat{\xi}^i, \tag{23}$$

with S being the implicitly defined selection matrix.

V. Robustness of ambiguity resolution over measurement biases

The float ambiguity estimates are fixed to integers if the float solution is sufficiently accurate. The covariance matrix of the float ambiguities is obtained from Eq. (22) and (23):

$$\Sigma_{\hat{N}^i_{ur}} = S\left((H^i)^{\mathrm{T}}\Sigma^{-1}_{z^i}H^i\right)^{-1}S^{\mathrm{T}}. \tag{24}$$

The float ambiguity estimates are decorrelated to increase the success rate of sequential fixing. The decorrelation is obtained from the triangular decomposition of the float ambiguity covariance matrix (see Golub and Van Loan [5]), i.e.

$$\Sigma_{\hat{N}^i_{ur}} = L^i_{ur}D^i_{ur}(L^i_{ur})^{\mathrm{T}}, \tag{25}$$

with L^i_{ur} being a lower triangular matrix and D^i_{ur} being a diagonal matrix. The decorrelated ambiguity estimates might be biased due to a measurement bias b_{z^i}, which propagates into the decorrelated ambiguities according to Eq. (22) - (25):

$$b_{\tilde{\hat{N}}^i_{ur}} = (L^i_{ur})^{-1}S\left((H^i)^{\mathrm{T}}\Sigma^{-1}_{z^i}H^i\right)^{-1}(H^i)^{\mathrm{T}}\Sigma^{-1}_{z^i}b_{z^i}. \tag{26}$$

The (unknown) measurement bias is assumed to be zero-mean Gaussian distributed with covariance matrix $\Sigma_{b_{z^i}}$. We believe that this is a quite reasonable assumption since smaller biases are typically more likely than larger biases.

The success rate of sequential ambiguity fixing can be determined in closed form for deterministic biases (see [1]) since the decorrelated ambiguities are statistically independent. However, the computation becomes more demanding if the ambiguity biases are themselves stochastic parameters. In this case, the success rate of sequential ambiguity fixing becomes:

$$P_{\text{suc}}^{i} = \prod_{j=1}^{K} \int_{b_{\tilde{N}_{ur}^{jl,i}}} p(b_{\tilde{N}_{ur}^{jl,i}}) \int_{-0.5}^{+0.5} p(\varepsilon_{\tilde{N}_{ur}^{jl,i}}, b_{\tilde{N}_{ur}^{jl,i}}) d\varepsilon_{\tilde{N}_{ur}^{jl,i}} db_{\tilde{N}_{ur}^{jl,i}}, \tag{27}$$

with $\varepsilon_{\tilde{N}_{ur}^{jl,i}}$ being the noise and $b_{\tilde{N}_{ur}^{jl,i}}$ being the bias of the j-th decorrelated float ambiguity. The probability distribution of the ambiguity bias is obtained from Eq. (26) as

$$p\left(b_{\tilde{N}_{ur}^{jl,i}}\right) = \mathcal{N}\left(0, (\Sigma_{b_{\tilde{N}_{ur}^{i}}})_{jj}\right), \tag{28}$$

with

$$\begin{aligned}\Sigma_{b_{\tilde{N}_{ur}^{i}}} = {} & (L_{ur}^{i})^{-1} S \left((H^{i})^{\mathrm{T}} \Sigma_{z^i}^{-1} H^{i}\right)^{-1} (H^{i})^{\mathrm{T}} \Sigma_{z^i}^{-1} \Sigma_{b_{z^i}} \\ & \Sigma_{z^i}^{-1} H^{i} \left((H^{i})^{\mathrm{T}} \Sigma_{z^i}^{-1} H^{i}\right)^{-1} S^{\mathrm{T}} ((L_{ur}^{i})^{-1})^{\mathrm{T}}. \end{aligned} \tag{29}$$

The probability distribution of the ambiguity error is given by

$$p\left(\varepsilon_{\tilde{N}_{ur}^{jl,i}}, b_{\tilde{N}_{ur}^{jl,i}}\right) = \mathcal{N}\left(b_{\tilde{N}_{ur}^{jl,i}}, (D_{ur}^{i})_{(j,j)}\right). \tag{30}$$

VI. Simulation Results

In this section, the performance of the proposed cascaded RTK positioning is evaluated with simulated Galileo measurements. The positions of the Galileo satellites are modeled according to the nominal full Walker constellation with 27 satellites in 3 orbital planes [6]. The receiver location is assumed to be in Munich, Germany, at 48.148841° N latitude and 11.570333° E longitude. The standard deviation of the (undifferenced) phase noise is considered to be 5 mm. The elevation mask is set to 5°. The measurement rate is 5 Hz.

Fig. 1 shows the positioning precision of the 2nd and 3rd cascade (as described in section IV): The ambiguity-fixed C1/C4 solution has an instantaneous precision between 40 cm and 80 cm depending on the satellite geometry, which improves to 10 to 20 cm within 30 epochs. The fixed C1/C2 solution shows an instantaneous precision of 5 to 10 cm.

Fig. 2 shows the robustness of ambiguity resolution with respect to uncorrected geometric and ionospheric biases. A success rate of more than 90 % is achieved for both combinations within 10 epochs (2 s). The C2 combination achieves a higher success rates than the C4 combination for unbiased measurements due to the lower noise amplification. The C4 combination becomes more attractive than the C2 combination if geometric and ionospheric biases exceed a certain level.

VII. Conclusion

We presented a cascaded Real-Time Kinematic (RTK) positioning method with multi-frequency linear combinations of carrier phase measurements. The simulation results for Galileo show that a robust ambiguity resolution can be obtained within a few epochs even if uncorrected geometric and ionospheric biases are in the order of several decimeters. The proposed method might be attractive for any application where reliability is more important than accuracy, e.g. autonomous driving.

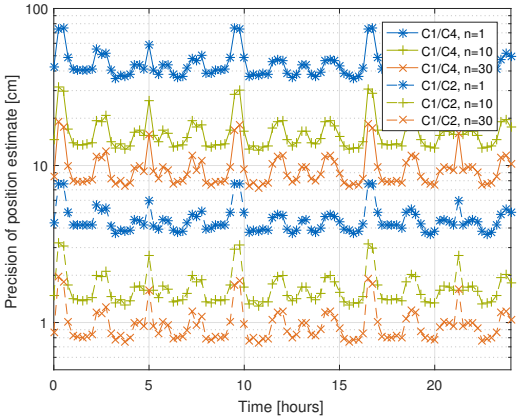

Figure 1. Precision of cascaded RTK positioning: The fixed C1/C4 solution has an instantaneous precision between 40 cm and 80 cm depending on the satellite geometry. The precision improves to 10 to 20 cm within 30 epochs. The fixed C1/C2 solution has a much higher precision.

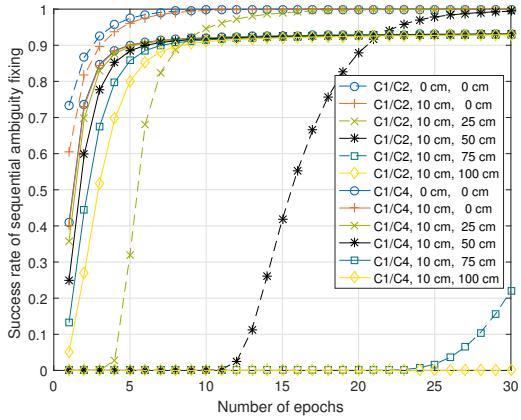

Figure 2. Robustness of ambiguity resolution with respect to uncorrected geometric and ionospheric biases: The legend shows the pair of considered combinations, the geometry bias and the ionospheric bias on E1. The first combination is always the C1 (Super-Wide-Lane) combination with resolved ambiguities. The success rates refer to the 2nd combination (C2 or C4).

References

[1] P. Teunissen, "Integer estimation in the presence of biases," *Journal of Geodesy*, vol. 75, no. 7-8, pp. 399–407, 2001.

[2] P. Henkel and C. Günther, "Three frequency linear combinations for Galileo," in *Proc. of 4th Workshop on Positioning, Navigation and Communication Symp. (WPNC)*, pp. 239–245, IEEE, 2007.

[3] P. Henkel and A. Sperl, "Precise RTK Positioning with GPS/INS Tight Coupling and Multipath Estimation," in *Proc. of the Intern. Techn. Meet. of the Inst. of Navigation (ION ITM), Monterey, USA*, pp. 1015–1023, 2016.

[4] J. Jung, P. Enge, and B. Pervan, "Optimization of cascade integer resolution with three civil GPS frequencies," in *Proc. of ION GPS*, pp. 2191–2200, 2000.

[5] G. H. Golub and C. F. Van Loan, "Matrix computations," *Johns Hopkins University, Press, Baltimore, MD, USA*, p. 723 pp., 1996.

[6] R. Zandbergen, S. Dinwiddy, J. Hahn, E. Breeuwer, and D. Blonski, "Galileo orbit selection," in *Proc. of 17th Intern. Techn. Meet. of the Inst. of Navigation (ION GNSS)*, pp. 616–623, 2004.